A MicroRNA Targeting Dicer for Metastasis Control

ARTICLE *in* CELL · JUNE 2010

Impact Factor: 32.24 · DOI: 10.1016/j.cell.2010.05.017 · Source: PubMed

Cell

A MicroRNA Targeting Dicer for Metastasis Control

Graziano Martello,[1] Antonio Rosato,[2,3] Francesco Ferrari,[4] Andrea Manfrin,[1] Michelangelo Cordenonsi,[1] Sirio Dupont,[1] Elena Enzo,[1] Vincenza Guzzardo,[5] Maria Rondina,[2] Thomas Spruce,[6] Anna R. Parenti,[5] Maria Grazia Daidone,[7] Silvio Bicciato,[4] and Stefano Piccolo[1,*]

[1]Department of Histology, Microbiology and Medical Biotechnologies, University of Padua School of Medicine, viale Colombo 3, 35126 Padua, Italy

[2]Department of Oncology and Surgical Sciences, University of Padua, via Gattamelata 64, 35126 Padua, Italy

[3]Istituto Oncologico Veneto, via Gattamelata 64, 35126 Padua, Italy

[4]Center for Genome Research, Department of Biomedical Sciences, University of Modena and Reggio Emilia, via G. Campi 287, 41100 Modena, Italy

[5]Department of Medical Diagnostic Science and Special Therapies, Section of Pathology, University of Padua, viale Gabelli 2, 35126 Padua, Italy

[6]Molecular Embryology Group, MRC Clinical Sciences Centre, Imperial College London, Hammersmith Hospital Campus, London W12 ONN, UK

[7]Department of Experimental Oncology, National Cancer Institute, via Venezian 1, 20133 Milan, Italy

*Correspondence: piccolo@bio.unipd.it

DOI 10.1016/j.cell.2010.05.017

SUMMARY

Although specific microRNAs (miRNAs) can be upregulated in cancer, global miRNA downregulation is a common trait of human malignancies. The mechanisms of this phenomenon and the advantages it affords remain poorly understood. Here we identify a microRNA family, *miR-103/107*, that attenuates miRNA biosynthesis by targeting Dicer, a key component of the miRNA processing machinery. In human breast cancer, high levels of *miR-103/107* are associated with metastasis and poor outcome. Functionally, *miR-103/107* confer migratory capacities in vitro and empower metastatic dissemination of otherwise nonaggressive cells in vivo. Inhibition of *miR-103/107* opposes migration and metastasis of malignant cells. At the cellular level, a key event fostered by *miR-103/107* is induction of epithelial-to-mesenchymal transition (EMT), attained by downregulating *miR-200* levels. These findings suggest a new pathway by which Dicer inhibition drifts epithelial cancer toward a less-differentiated, mesenchymal fate to foster metastasis.

INTRODUCTION

microRNAs (miRNAs) are an evolutionarily conserved group of small RNAs (18–24 nucleotides) that inhibit gene expression. miRNAs are transcribed by RNA polymerase II as longer precursors and then processed into mature miRNAs by the sequential action of Drosha and Dicer endonucleases (Bartel, 2009). Mature miRNAs operate via sequence-specific interactions with the 3′ untranslated region (UTR) of cognate mRNA targets, causing suppression of translation and mRNA decay (Ambros, 2004; Bartel, 2009).

miRNAs coordinate the expression of entire sets of genes, shaping the mammalian transcriptome (Bartel, 2009). Loss of miRNA biosynthesis, as in *Dicer* knockouts, is lethal, owing to mitotic catastrophe and severely defective stem cell proliferation and differentiation (Bernstein et al., 2003; Fukagawa et al., 2004; Tang et al., 2007).

A large body of evidences suggests that the multigene regulatory capacity of miRNAs is dysregulated and exploited in cancer: miRNA loci are targeted by genetic and epigenetic defects, and miRNA "signatures" have been found informative for tumor classification and clinical outcome (Calin and Croce, 2006; Ventura and Jacks, 2009).

Although several miRNAs are upregulated in specific tumors (Volinia et al., 2006), a global reduction of miRNA abundance appears a general trait of human cancers, playing a causal role in the transformed phenotype (Kumar et al., 2007; Lu et al., 2005; Ozen et al., 2008). However, little is known on the underlying mechanisms or the phenotypic advantages afforded to cells by reduced miRNA expression and, if any, on the clinical relevance of this phenomenon. The present work sheds light on these questions as here we identify a microRNA family, *miR-103/107*, whose expression is associated with metastasis and poor outcome in breast cancer patients. *miR-103/107* inhibit the expression of Dicer, causing global microRNA downregulation. *miR-103/107* foster the acquisition of mesenchymal characteristics and are relevant for breast cancer cell migration and metastatic dissemination.

RESULTS

miR-103/107 Target Dicer

miRNAs constrain gene expression by binding to the 3′UTR of messenger RNA (mRNAs); thus, genes that must remain active

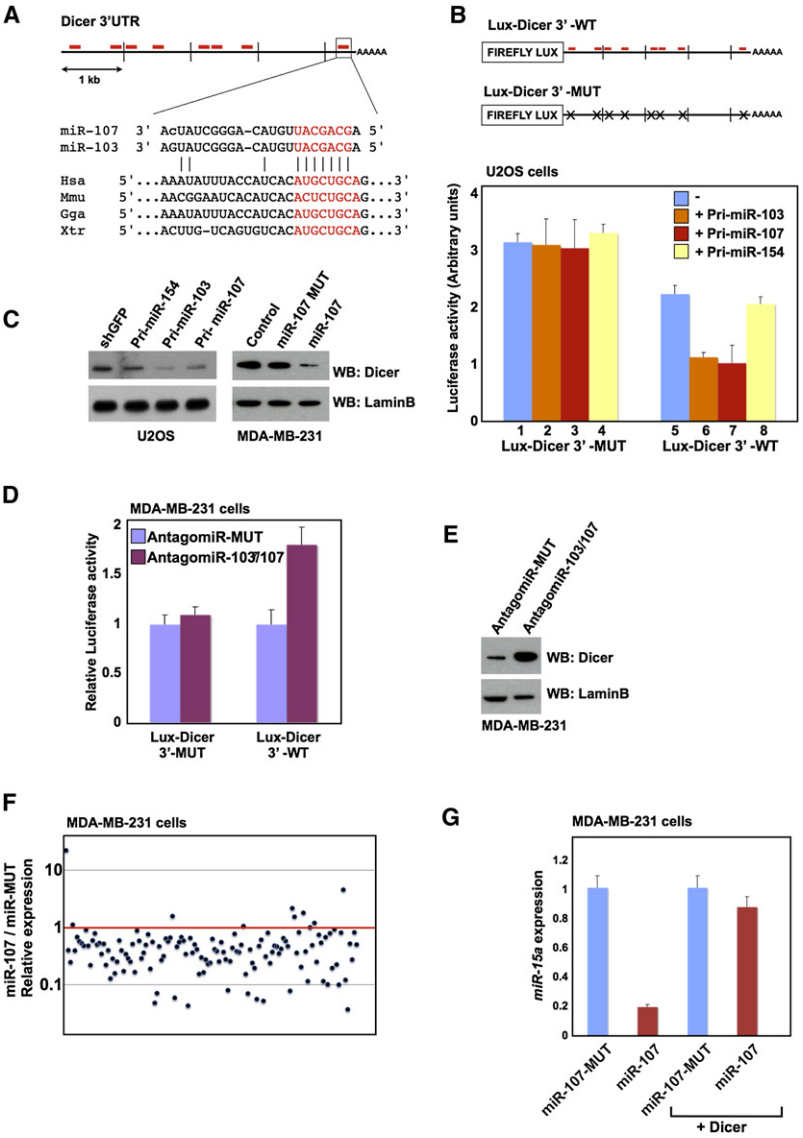

Figure 1. *miR-103/107* Target Dicer

(A) Schematic representation of the 3′UTR of *Dicer*. Red bars show predicted *miR-103/107* target sequences. Below, sequences of mature *miR-103* and *miR-107* aligned to one of these target sites, revealing evolutionary conservation in the seed-pairing sequence between amphibians (*Xenopus*, Xtr), birds (*Gallus*, Gga), and mammals (human, Hsa and mouse, Mmu).

(B) Schematic representation of the reporters for *miR-103/107* activity against the *Dicer* 3′UTR. The CMV promoter drives constitutive transcription of a chimeric mRNA containing the firefly *luciferase* coding sequence fused to the full-length *Dicer* 3′UTR (Lux-Dicer-3′-WT) or to the same UTR mutated in all the *miR-103/107* seed-pairing sequences (Lux-Dicer-3′-MUT). Below, the predicted *miR-103/107*-binding sites in the 3′UTR of *Dicer* mRNA are responsive to endogenous (compare lane 1 with lane 5) and overexpressed *miR-103* or *miR-107* in human U2OS cells. Luciferase reporters were transfected in parental (–) or in stable cell lines expressing *pri-miR-103*, *pri-miR-107*, or, as a control, the unrelated *pri-miR-154*. Absolute values are shown as mean and standard deviation (SD).

(C) Downregulation of endogenous Dicer protein expression by *miR-103/107* as assayed by immunoblotting. LaminB serves as loading control. Controls are shGFP (U2OS) or scrambled siRNA (MDA-MB-231). Mature *miR-107*-MUT bears mutations in the seed sequence and is inactive compared to wild-type.

(D and E) Endogenous requirement of *miR-103/107* as Dicer inhibitors. In (D), bars show expression of the *Dicer* 3′UTR reporters in cells depleted of endogenous *miR-103/107* by treatment with antagomiR. Values relative to antagomiR-MUT-treated cells are shown as mean and SD. Effectiveness and specificity of antagomiR treatments on endogenous *miR-103/107* expression are shown in Figure S1D. In (E), endogenous Dicer protein levels are upregulated in *miR-103/107*-depleted cells.

(F) In line with its effect on Dicer, overexpression of *miR-107* causes a global reduction of mature miRNAs endogenously expressed in MDA-MB-231 cells. Dots show the ratio of miRNAs expression levels in *miR-107* versus *miR-107*-MUT transfected cells. Global miRNA expression was measured with TaqMan Human miRNA Array and normalized to *snRNA-U6b* loading control. See Table S1 for expression values.

(G) Expression of a *miR-103/107*-insensitive *Dicer* cDNA rescues mature miRNA expression, here exemplified by *miR-15a*. The effects of *miR-107* on mature *miR-15a* levels were compared in parental and MDA-MB-231 cells stably expressing a *miR-103/107*-insensitive form of Dicer (+Dicer). *miR-15a* expression was measured by qRT-PCR and normalized to *snRNA-U6b* loading control. Relative values are shown as mean and SD.

See also Figure S1 and Table S1.

across different cell types, such as housekeeping genes, typically evolved 3′UTRs that are short, allowing them to escape this regulation (Bartel, 2009). During a survey of the 3′UTRs of several housekeeping genes, we were struck by the unusual length of the 3′UTR of *Dicer* (>4000 bp). As Dicer is essential for processing miRNA precursors (Filipowicz et al., 2008), this raised the possibility that some mature miRNAs could feed back to control Dicer expression. To explore this further, we used Pictar and TargetScan computational tools (Friedman et al., 2009; Krek et al., 2005) to search for miRNA binding sites in the 3′UTR of *Dicer*. From this analysis, the *miR-103/107* family (composed of *miR-103.1, miR-103.2*, and *miR-107)* stood out for the presence of eight evolutionarily conserved binding sites, suggesting cooperative binding and biologically effective interaction (Figure 1A).

To test if *miR-103/107* target Dicer, we first generated reporter constructs in which the full-length 3′UTR of *Dicer*, either wild-type or mutant in the *miR-103/107*-binding sites, was cloned downstream of the luciferase open reading frame (Lux-Dicer-3′-WT or -MUT, respectively, Figure 1B). The activity of these two reporters was compared in human U2OS cells: the wild-type reporter showed a reduced expression compared to its mutant version, as expected if the endogenous *miR-103/107* were pairing to the predicted binding sites (Figure 1B, compare lanes 1 and 5). Retroviral transduction of either *pri-miR-103* or *pri-miR-107* expression vectors caused further inhibition of the wild-type

3′UTR reporter (Figure 1B, compare lane 5 with lanes 6 and 7) but not of the corresponding seed mutant reporter. As control, forced expression of the unrelated *pri-miR-154* or *shGFP* had no effect on luciferase expression (Figure 1B, lane 8). Collectively, these data indicate that *miR-103/107* target the *Dicer* 3′UTR.

We next monitored to what extent *miR-103/107* affect the endogenous levels of Dicer protein. In multiple cell lines, Dicer protein was specifically downregulated (about 50%–60% reduction) by expressing *pri-miR-103* or *pri-miR-107* (Figure 1C, left panel and Figure S1A available online). To exclude any potentially confounding effect from the viral expression system—or from flanking sequences of the pri-miR constructs—we also transiently transfected cells with the mature form of *miR-107* or, as control, a mutant *miR-107* that contained three mismatches in the seed-binding sequence (*miR-107*-MUT). Dicer protein levels were downregulated by mature *miR-107* but not *miR-107*-MUT (Figure 1C, right panel and Figure S1B). *miR103/107* affect Dicer levels acting on its 3′UTR, as lentiviral expression of Dicer lacking the 3′UTR was insensitive to *miR-107* (Figure S1C).

Next, we tested if *miR-103/107* are causal for Dicer downregulation in a loss-of-function experimental setting. For this, we used antagomiR reagents (Krutzfeldt et al., 2005) to silence endogenous *miR-103/107* (antagomiR-103/107); as a control, we used a mutant version of this reagent carrying six mismatches (antagomiR-MUT) (Figure S1D). As shown in Figure 1D, treatment of MDA-MB-231 cells with antagomiR-103/107 specifically promoted expression of the *Dicer* 3′UTR-wild-type reporter and, crucially, upregulated endogenous Dicer protein, as assayed by immunoblotting (Figure 1E). Thus, Dicer levels are limited by endogenous *miR-103/107*.

We then investigated the effects of the *miR-103/107*-Dicer interaction on miRNA biosynthesis, by comparing miRNAs levels in MDA-MB-231 cells expressing *miR-107* or *miR-107*-MUT. As assayed quantitatively by qPCR, mature miRNAs were globally downregulated in the presence of *miR-107*, and this is phenocopied by Dicer knockdown (Figure 1F; Figures S1E and S1F; and Table S1). Sustaining Dicer expression by means of a *miR-107*-insensitive transgene rescues this effect (Figure 1G, Figure S1G, and data not shown).

If *miR-103/107* restrict miRNA processing at the level of Dicer, then the levels of *miR-103/107* should directly correlate with the abundance of Dicer substrate, that is, the 70 nt precursor miRNAs (pre-miRNAs). Indeed, pre-miRNAs, but not pri-miRNAs, accumulate in *miR-107*-expressing MDA-MB-231 cells (Figure S1H).

In sum, *miR-103/107* lead to inhibition of miRNA biogenesis through Dicer downregulation.

Inverse Correlation between *miR-103/107* and Dicer Levels in Cancer Cell Lines

At this point, we were intrigued by the analogy between the effects of *miR-103/107* on Dicer function and the hampered maturation of multiple miRNAs observed in human tumors (Lu et al., 2005; Ozen et al., 2008; Ventura and Jacks, 2009). Following this lead, we first compared the endogenous levels of *miR-103/107* and Dicer protein in a well-established cellular model of mammary tumor progression, consisting of four distinct cell lines, 67NR, 168FARN, 4TO7, and 4T1, all derived from a single primary tumor and whose activity as xenografts reflects the sequence of multistep progression toward metastasis (Aslakson and Miller, 1992). We found that *miR-103/107* expression levels increased from the nonaggressive cells (67NR, 168FARN) to metastatic lines (4TO7 and 4T1). Conversely, endogenous Dicer protein levels decreased in metastatic lines (Figure 2A). To determine whether the expression of *miR-103/107* increases with enhanced metastatic propensity in another cellular context, we analyzed SW480 and SW620 human colon cancer cell lines, derived, respectively, from the primary tumor and a metastasis of the same patient (Leibovitz et al., 1976). As shown in Figure 2B, an inverse correlation between *miR-103/107* and Dicer level could also be observed in this case.

Clinical Association of *miR-103/107* Expression to Breast Cancer Metastasis and Poor Prognosis

The data on cell lines suggested a possible link between *miR-103/107* expression and tumor progression. We surmised that, if biologically meaningful, this mechanism might also be found in human tumors. For this, we measured mature *miR-103/107* levels in a collection of breast cancer patients treated in our Institution with annotated clinical history. Patients were divided in two groups, with respectively high or low levels of *miR-103/107* (Figure 2C, see Extended Experimental Procedures). Remarkably, when tested using the Kaplan-Meier survival analysis, the *miR-103/107* "high" group displayed a significant higher probability to develop metastasis when compared to the "low" group (Figure 2D). In line with our biochemical characterization of Dicer as target of *miR-103/107*, the "high" group tumors showed a reduced level of Dicer protein when compared to the "low" group, as assayed by immunohistochemisty (Figures 2E–2H).

We next wished to extend these analyses to independent cohorts of patients. For this, we took advantage of the fact that *miR-103* and *miR-107* are intronic miRNAs contained in three *PANK* (Pantothenate kinase) loci of the human genome (i.e., *PANK1*, *2*, and *3* corresponding to *pri-miR-107*, *pri-miR-103-2*, and *pri-miR-103*-1, respectively). Expressions of *PANK* genes paralleled that of *miR-103/107* in the series of cell lines described above (Figure S2); this coexpression is in line with a previous analysis in normal human tissues (Baskerville and Bartel, 2005).

We thus used *PANK/pri-miR-103/107* expression as an approximation of *miR-103/107* levels to interrogate several public gene expression datasets for which a wealth of molecular and associated clinical data is available (summing up to more than 1000 breast cancer patients, see Extended Experimental Procedures). For each dataset, tumors were divided in two groups, with respectively high or low levels of *pri-miR-103/107* (see Extended Experimental Procedures for details). In agreement with our previous analyses on mature *miR-103/107*, the group expressing higher levels of *pri-miR-103/107* displayed a significantly higher probability to develop metastasis and poor outcome when compared to the "low" group (Figure 2I and Figure S3). Taken together, our results suggest that high *miR-103/107* expression is unlikely to represent a general feature of all tumors but rather identifies those associated to adverse and metastatic disease.

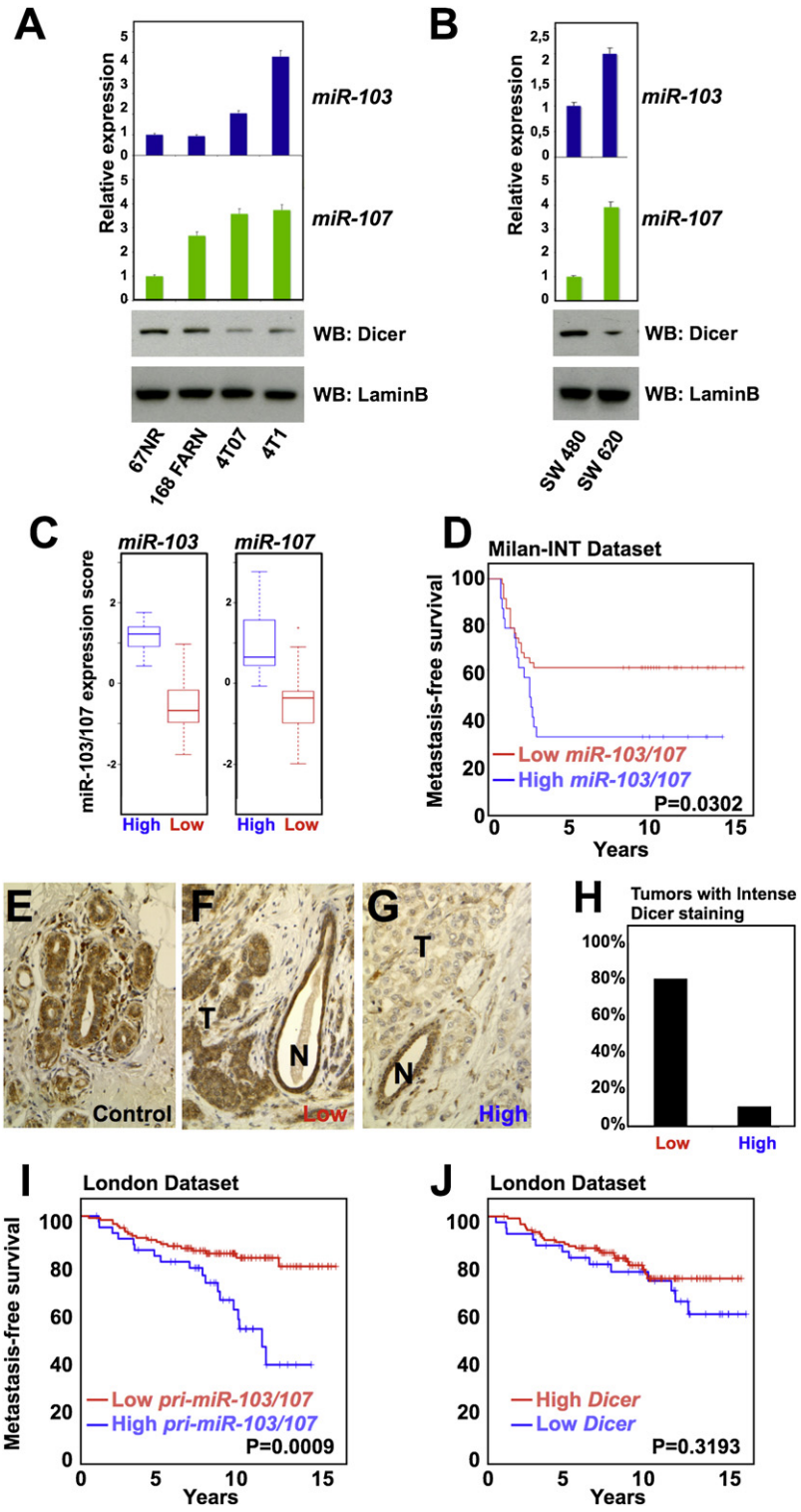

Figure 2. Clinical Association of *miR-103/107* with Metastasis in Breast Cancer Patients

(A and B) Top panels: Expression of *miR-103/107* increases in cellular models of metastasis progression, as assayed by qRT-PCR. Values relative to the nonmetastatic, less aggressive line (67NR and SW480, respectively) are normalized to *snRNA-U6b* and shown as mean and SD. Lower panels: Western blot for Dicer showing the inverse correlation between Dicer protein levels and *miR-103/107* expression. LaminB serves as loading control. See also Figure S2 for levels of *pri-miR-103/107* in the same samples.

(C and D) Mature *miR-103/107* levels predict metastasis proclivity in breast cancer patients.

(C) Box plots showing the expression levels of mature *miR-103* and *miR-107* in breast cancer samples from the "Milan-INT" patients' dataset (Table S2). Samples were divided in two groups with coherent low or high expression of both genes. "Low" and "High" are the names of the two groups of patients. Each box represents median and 75th and 25th percentile values.

(D) Kaplan-Meier graph representing the probability of metastasis-free survival in breast cancer patients from the "Milan-INT" dataset stratified as in (C). The log-rank test p value reflects the significance of the association between high *miR-103/107* levels and metastasis.

(E–H) Immunohistochemistry for Dicer protein expression in primary human breast cancer samples from the "Milan-INT" dataset (analyzed above). Panels show representative pictures of Dicer staining in normal breast tissue (E) or cancer tissues with low (F) or high (G) levels of *miR-103/107* ("Low" and "High" groups, respectively). N indicates mammary ducts with normal morphology (used as internal positive controls for Dicer IHC), whereas T indicates tumor cells. (H) Percentage of breast cancer samples (n = 20), from the "Low" and "High" groups, that display Dicer staining in the cancer tissue comparable to the adjacent normal tissue (as shown in F).

(I and J) Kaplan-Meier graphs representing the probability of metastasis-free survival in breast cancer patients from the "London" dataset (see Extended Experimental Procedures) stratified according to low or high *pri-miR-103/107* expression levels (I) or to low and high *Dicer* expression levels (J). The log-rank test p values reflect the significance of the association between high *pri-miR-103/107* and metastatic relapse but fail to show any association for *Dicer*. See Figure S3 for similar results obtained from four other independent breast cancer datasets.

Given the significant association between *miR-103/107* expression, Dicer protein levels, and clinical relapse, we wished to establish if a similar association existed for *Dicer* transcripts. However, when breast cancer patients' stratification was repeated based on high or low *Dicer* mRNA levels, our analyses failed to detect a significant association with metastasis or outcome (Figure 2J and Figure S3).

miR-103/107 Downregulate Dicer to Promote Cell Migration and Invasion In Vitro

In light of the preceding data, we sought to determine more directly if the *miR-103/107*-Dicer connection plays a causal role in conferring aggressive traits to breast cancer cells. For this, we assayed how gain or loss of function of either *miR-103/107* or Dicer impacted on cell migration, a hallmark of metastatic capacity. We first assayed 168FARN and SUM149: these cells are tumorigenic but

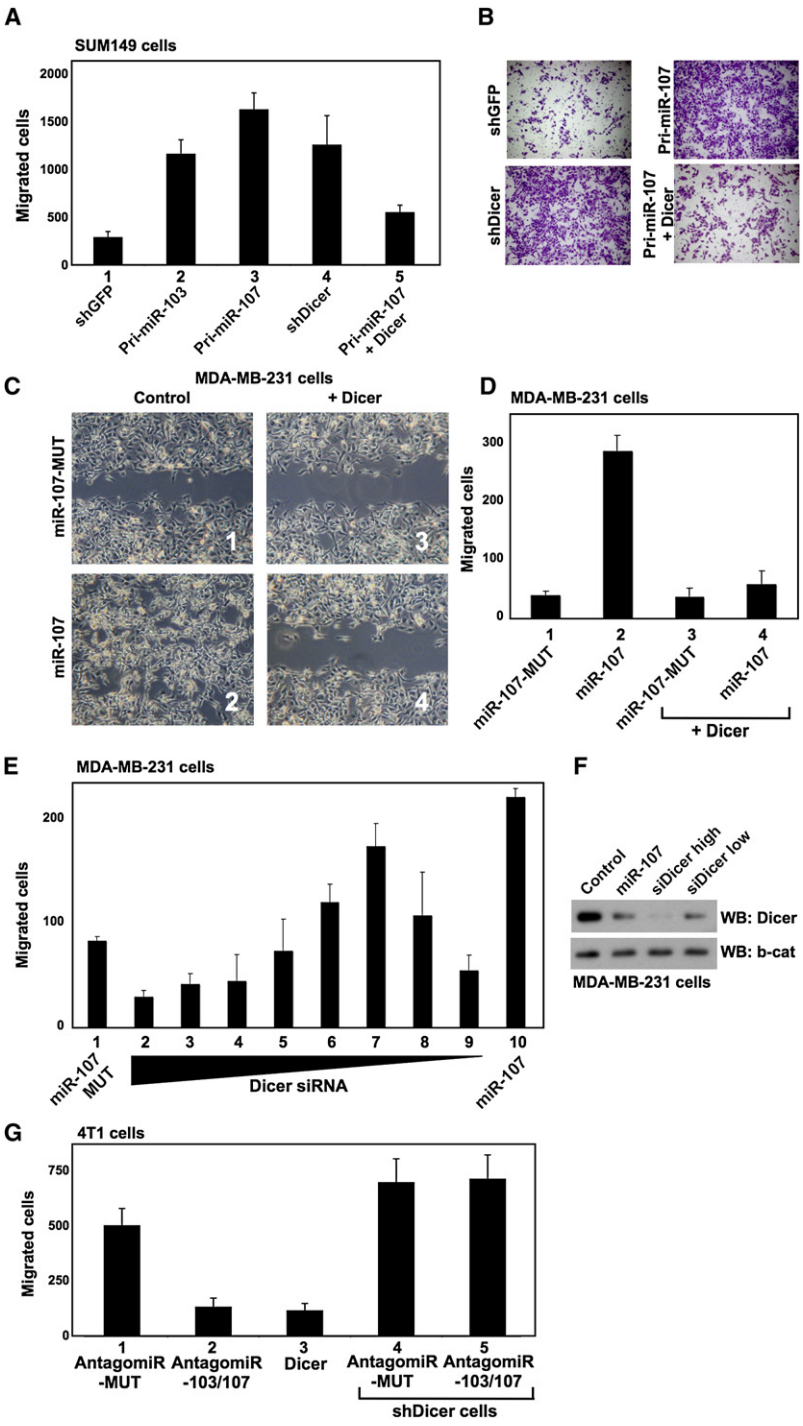

Figure 3. *miR-103/107* Outbalance Dicer to Promote Cell Migration and Invasion

(A and B) *miR-103/107* expression promotes migration in SUM149 breast cancer cells by attenuating Dicer levels. Stable cell lines expressing shGFP (lane 1), *pri-miR-103* (lane 2), *pri-miR-107* (lane 3), and shDicer (lane 4) from retroviral expression vectors were compared in transwell migration assays. Lane 5 shows the effect of a miR-insensitive Dicer transgene on migration of cells already expressing *pri-miR-107*. (A) absolute quantifications of cells migrated through the transwell. (B) representative pictures of cells migrated through the filter, stained with crystal-violet, taken at the same magnification (5×).

(C and D) *miR-107* promotes migration of parental MDA-MB-231 breast cancer cells (Control) but not of cells expressing miR-insensitive *Dicer* (+Dicer). Graph in (D) shows the absolute number of cells invading the wound for which we provide representative pictures in (C).

(E) Wound-healing assay as in (C) showing how only partial knockdown of Dicer (lanes 6–8) mimics gain of *miR-107* to promote cell migration. MDA-MB-231 cells were transfected with 2-fold serial dilutions of Dicer siRNA, ranging from 25 nM (lane 2) to 0.2 nM (lane 9). Graphs show the absolute number of cells invading the wound.

(F) Immunoblotting of cells transfected as in (E). siDicer high (25 nM) corresponds to lane 2, siDicer low (0.8 nM) to lane 7. Note comparable depletion between the latter and *miR-107*. β-catenin (b-cat) serves as loading control.

(G) Endogenous *miR-103/107* promote cell migration through Dicer downregulation. Depletion of endogenous *miR-103/107* by treatment with antagomiR-103/107 reduces the migration of 4T1 cells (lanes 1 and 2), without having effect on proliferation and cell cycle (see Figure S4E). Stable expression of Dicer similarly opposes cell migration (lane 3). In contrast, migration of Dicer-depleted cells (shDicer) is not reduced by treatment with antagomiR-103/107 (compare lanes 4 and 5). Graphs show the absolute quantitations of cells invading transwell filters.

Data are represented as mean and SD. See also Figure S4.

display poor migratory capacities and contain relatively low levels of *miR-103/107* (see Figure 2A and data not shown). As assayed in transwell migration assays, raising *miR-103/107* in these cell lines increased migration by 8- to 10-fold, whereas overexpression of control-shGFP had no effect (Figure 3A, compare lane 1 with lanes 2 and 3, Figure 3B. See Figure S4A for results on 168FARN cells).

Induction of migratory capacity by *miR-103/107* relies on attenuation of Dicer as expression of *miR-103/107* is phenocopied by shDicer SUM149 cells (reducing Dicer to about 40% its normal levels) and is rescued by coexpression of a miR-insensitive *Dicer* transgene that restores Dicer protein to a level near-to-endogenous (Figure 3A, lanes 4 and 5, see immunoblots in Figure S4C). Similar results were obtained in wound-healing assays with another, more aggressive cell line, MDA-MB-231 cells (Figures 3C and 3D). Thus, *miR-103/107* empower cell motility through Dicer inhibition.

Complete loss of Dicer is detrimental for cell survival (Fukagawa et al., 2004), whereas here we show that *miR-103/107* enhance motility with no effect on cell proliferation (Figures S4B and S4D). Different degrees of Dicer downregulation may reconcile these findings, as Dicer protein is only partially downregulated by *miR-103/107*. To tackle this quantitative issue, we transfected MDA-MB-231 cells with increasing doses of *Dicer*

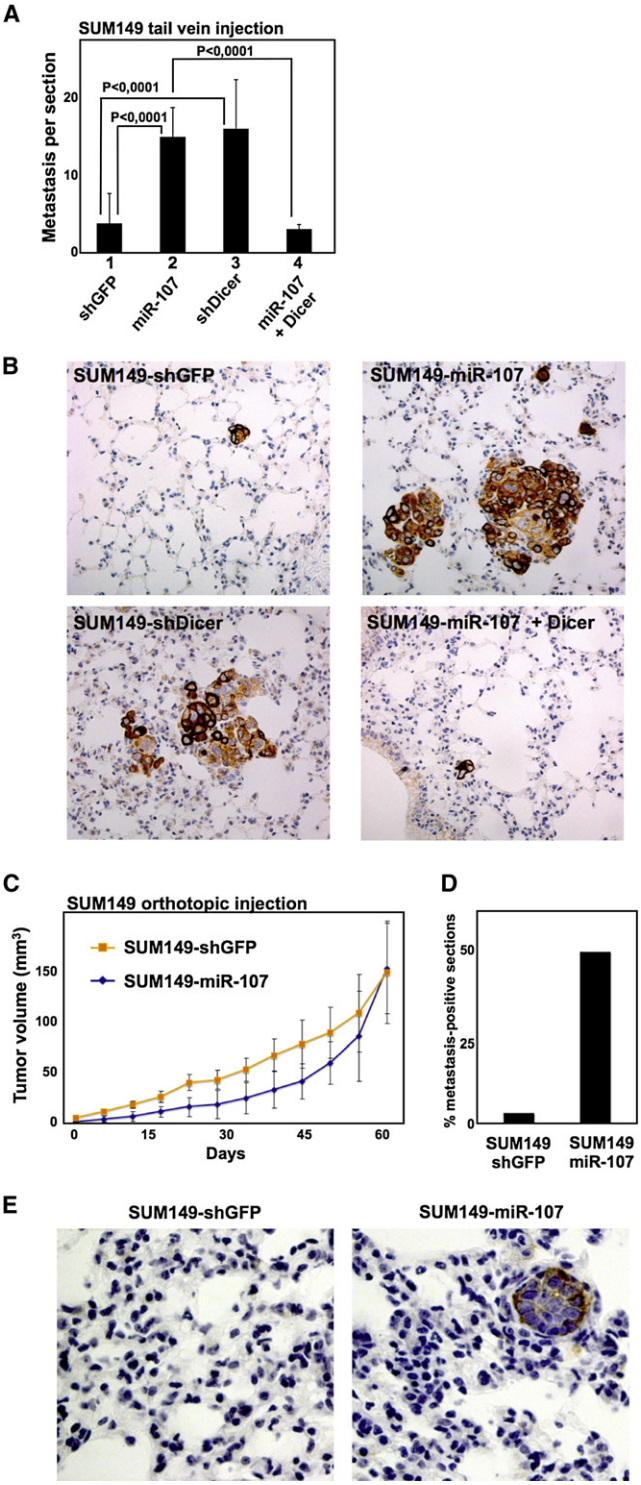

Figure 4. *miR-107* Induces Metastatic Dissemination

(A and B) Lung colonization assays of SUM149 derivatives after injection in the tail vein of SCID mice (8 mice per cell line). Four weeks after injection, lungs were analyzed for the presence of metastatic nodules.

(A) Quantification of metastatic nodules formed by the indicated SUM149 derivatives. Analyses were carried out on histological sections of the lungs (4 sections per lung) stained with the anti-cytokeratin antibodies AE1/AE3. Data are represented as mean and SD.

(B) Representative pictures of metastases embedded in the lung parenchyma. Macrometastases were observed only in mice injected with cells expressing *pri-miR-107* or shDicer.

(C) SCID mice were orthotopically injected in the fat pad with SUM149-shGFP or SUM149-*miR-107* cells. The rates of primary tumor growth were not significantly different, showing, if anything, a reduced proliferation of SUM149-*miR-107* in vivo. Data are represented as mean and SD.

(D and E) *Pri-miR-107* promotes distant metastatic dissemination of breast cancer cells from the orthotopic site. Lungs of mice injected in (C) were explanted after 12 weeks and scored for the presence of metastases as in (A). (E) Right panel: representative metastatic focus of SUM149-*miR-107* cells embedded in the lung parenchyma. Graphs in (D) provide a quantification of metastatic dissemination measured as the percentage of sections displaying at least one metastasis out of n = 8 SUM149-shGFP injected mice and n = 8 SUM149-*miR-107* injected mice. Four to six serial sections were sampled and analyzed for each mouse.

siRNA, inducing a range of depletions, from negligible to more quantitative knockdown (Figure 3F and data not shown). As expected, full Dicer knockdown impaired cell viability and, consequently, secondarily reduced cell migration if compared to control cells (Figure 3E, compare lane 1 with lanes 2–4). Remarkably, however, partial attenuation of Dicer to levels similar to those achieved by *miR-103/107* (i.e., 50%–60% reduction) potently fostered cell migration (Figure 3E, lanes 6–8 and 10 and Figure 3F). Similar results were obtained with immortalized mouse mammary epithelial cells NMuMg (Figures S4F–S4H). These findings suggest that cell migration is exquisitely sensitive to the levels of Dicer, and that the degree of Dicer downregulation imposed by *miR-103/107* is sufficient to unleash aggressive cell behaviors.

We next tested if endogenous levels of *miR-103/107* are required for cell migration in the highly metastatic tumor cell line 4T1. For this, we first silenced *miR-103/107* by treatment with antagomiR-103/107. This leads to a 5-fold reduction in migratory properties similar to that one obtained by increasing Dicer expression (Figure 3G, lanes 1–3). Strikingly, loss-of-Dicer renders 4T1 cells insensitive to loss of *miR-103/107*, indicating that Dicer is epistatic to *miR-103/107* (Figure 3G, compare lanes 1 and 2 with lanes 4 and 5). Taken together, the data suggest that the balance between *miR-103/107* and Dicer is critical to controlling cancer cell motility.

Expression of *miR-107* Endows Metastatic Potential

The data presented so far raised the possibility that the link between *miR-103/107* and Dicer could configure in vivo a metastasis-promoter/suppressor pair. To test this idea, we assayed if *miR-103/107* could foster metastasis in vivo. For this, we used SUM149 cells, which form nonmetastatic primary tumors in vivo after injection in the mouse mammary gland (Ma et al., 2007) but retain residual lung colonization capacity when delivered through the tail vein. Notably, expression of *pri-miR-107*, but not shGFP (control), strongly promoted metastatic colonization (Figure 4A, compare lanes 1 and 2, and Figure 4B). In agreement with our previous in vitro characterization, this is phenocopied by partial depletion of Dicer (Figure 4A, lane 3 and Figure 4B). Conversely, rescuing Dicer expression (Figure S4C) abolished the prometastatic effects of *miR-107* (Figure 4A, lane

4 and Figure 4B). Thus, Dicer serves as metastasis suppressor downstream of *miR-103/107*.

Having established this relationship, we next asked whether *miR-107* would also empower distant metastatic dissemination from primary tumor masses. For this, we implanted control (shGFP) and *miR-107*-expressing SUM149 cells in the mammary fat pad of immunocompromised mice. As previously shown in vitro, gain of *miR-107* does not foster proliferation in vivo, not even within the competitive tumor microenviroment (Figure 4C). After 12 weeks, host mice were sacrificed and examined for the presence of metastatic lesions in the lung. Although no macroscopic metastases were detected, the staining of histological sections with anti-cytokeratin antibodies revealed the presence of micrometastatic foci in the lungs explanted from mice bearing the SUM149-*miR-107* xenografts, whereas almost none were found in mice injected with control cells (Figures 4D and 4E). Thus, once overexpressed, *miR-107* is a prometastatic factor that unleashes the ability to initiate distant dissemination in otherwise nonmetastatic cells. Further, these data provide functional support to the association between *miR-103/107* and clinical relapse previously revealed in human tumors.

Silencing of *miR-103/107* Inhibits Metastasis

We next asked if continuous repression of Dicer by endogenous *miR-103/107* in aggressive cells is required for metastatic spread in vivo. For this, 4T1 cells were injected into the mammary fat pad of recipient mice and tumors treated either with antagomiR-103/107 or antagomiR-MUT (see Experimental Procedures). As shown in Figure 5A, we found that the onset and size of primary tumors were comparable in the two groups of mice (p value > 0.05), despite the quantitative loss of endogenous mature *miR-103/107* in antagomiR-103/107-treated primary tumors (Figure 5B). Strikingly, however, although the antagomiR-MUT receiving cells invaded the lung parenchyma, silencing of *miR-103/107* efficiently reduced metastatic colonization (Figures 5C, 5D, and 5E). This occurred without detectable detrimental effects on normal mammary glands (Figure S5A). Thus, endogenous *miR-103/107* is critical for efficient metastatic dissemination of breast cancer cells.

We also compared control and *miR-103/107*-depleted primary tumors for expression of a number of miRNAs. As expected from the rescue of endogenous Dicer activity, silencing of *miR-103/107* enhanced global miRNA processing, as revealed by the increased levels of mature miRNAs (Figure 5F) and concomitant reduction of the 70 nt miRNA precursors (Figure S5B). This suggests that Dicer is limiting in metastatic tumors.

If the reduction of Dicer activity by high *miR-103/107* is critical for the execution of the metastatic program, then sustaining Dicer expression should phenocopy the loss of *miR-103/107* and oppose metastasis. To test this, we selected two Dicer-overexpressing 4T1 cell clones from a lentivirally infected cell population (Figure S5C). Dicer-4T1-derived tumors were strikingly deprived of metastatic capacity when compared to lesions from mock-infected cells (Figures 5G–5I). In sum, the data reveal a functional pathway in aggressive tumors, whereby endogenous *miR-103/107* are instrumental to attenuating Dicer levels below a threshold for metastasis protection.

Because levels of Dicer are around 50% when *miR-103/107* are elevated, one would expect that heterozygous loss of *Dicer* would represent one mechanism selected during tumor progression to favor metastasis. To explore this issue, we queried array CGH profiling of breast cancers and found that some tumors display a reduced copy number of the *Dicer1* locus, a finding compatible with *Dicer* heterozygosity; intriguingly, this subset of tumors also display an increased propensity to develop metastasis (Figure S5D). This provides a genetic proof-of-principle that selective pressure for Dicer downregulation exists in aggressive breast cancer. Interestingly, *pri-miR-103/107* expression levels are able to stratify patients according to outcome only in $Dicer^{+/+}$ tumors but not upon *Dicer* heterozygosity (Figure S5E). In other words, *Dicer* heterozygous tumors lost selective pressure for *miR-103/107* upregulation, supporting the notion that these molecules are indeed in the same pathway. It is, however, remarkable that the number of tumors displaying elevated *miR-103/107* and wild-type *Dicer* is higher (37%, n = 313) than those carrying copy-number variations of the *Dicer* gene (18%), suggesting that the use of an miRNA is preferred to genetic deletions, at least in this context (see Discussion).

miR-103/107 Promote Epithelial-to-Mesenchymal Transition

We next wished to understand the nature of aggressive cell behaviors leading to metastatic dissemination empowered by the *miR-103/107*-Dicer axis. We found that *miR-107* expression did not significantly affect cell proliferation, growth after serum starvation, resistance to apoptotic stimuli, and anoikis in immortalized mammary cell lines (MCF10A, NMuMG) or tumor cell lines (SUM149, MDA-MB231) (data not shown). This is in line with our previous measurements of the growth rates of cancer cells in vitro and in vivo upon gain or loss of *miR-103/107* (Figure 4C, Figure 5A, and Figures S4B, S4D, and S4E).

In contrast, our attention was attracted by a striking change in cellular shape promoted by overexpression of *miR-107*, whereby the cobblestone-like appearance of epithelial cells switched to a spindle-, fibroblast-like morphology with extensive cellular scattering and formation of lamellipodia (Figures 6A and 6B). These are hallmarks of epithelial-to-mesenchymal transitions (EMT). EMT is a pivotal cellular program to induce rapid changes in the shape and motility of epithelial cells, normally used during morphogenesis and tissue repair. EMT is also aberrantly activated in cancer cells to promote their malignant and stem cell characteristics (Polyak and Weinberg, 2009). The aggressive traits conferred by the EMT program to carcinoma cells presented clear similarities with those empowered by *miR-103/107*: both are clinically associated in breast cancer with poor clinical outcome and are functionally required for migration, invasion, and metastasis (Polyak and Weinberg, 2009).

To determine if the molecular alterations typical of an EMT occurred in *miR-107*-expressing cells, we examined the localization of adherent and tight junction markers, such as E-Cadherin and ZO-1 in NMuMg cells, a well-established model system for the study of EMT (Miettinen et al., 1994). Immunofluorescence showed that these proteins were strongly downregulated in cells

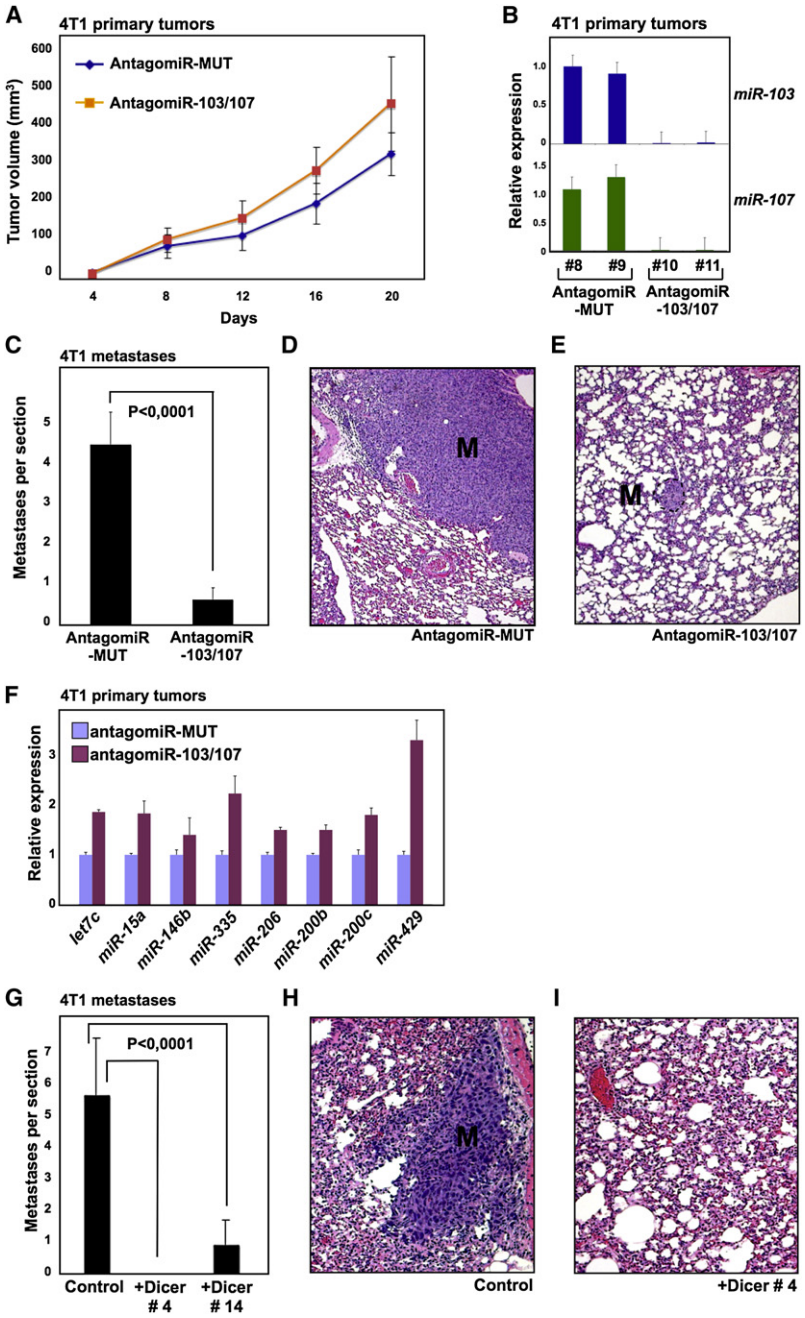

Figure 5. Endogenous Requirement of *miR-103/107* for Metastatic Dissemination

(A) The onset and growth rates of orthotopic 4T1 primary tumors were not significantly different in the presence (AntagomiR-MUT) or absence (AntagomiR-103/107) of *miR-103/107* expression. Data are represented as mean and SD.

(B) AntagomiR-103/107 inhibits *miR-103* and *miR-107* expression in 4T1-derived primary tumors formed upon orthotopic injection (fat pad) in SCID mice. Panels show expression levels of the indicated microRNAs as measured by qRT-PCR on representative primary tumors (explanted from mice dubbed #8 to #11), normalized to *snRNA-U6b* loading control. Data are represented as mean and SD of replicas.

(C) Depletion of *miR-103/107* reduces metastatic colonization. Lungs of mice injected in (A) were explanted after 21 days and scored for the presence of metastases. Metastatic burden was measured as the average number of metastatic foci per histological section (H&E stained), quantifying 10 to 12 serial sections for each mouse, on n = 10 mice for each regimen. p value was obtained using a one-sided Student's t test.

(D and E) Pictures show representative H&E sections of the lung parenchyma from 4T1 tumor-bearing mice treated with antagomiR-MUT (D) or antagomiR-103/107 (E). M, metastatic nodule.

(F) In vivo depletion of *miR-103/107* enhances miRNA maturation. Bars show the comparison between expression of the indicated mature miRNAs in antagomiR-MUT- versus antagomiR-103/107-treated 4T1 pooled primary tumors (n = 3 for each treatment), as measured by qRT-PCR. Relative values are shown as mean and SD. See Figure S5B for expression levels of the corresponding pre-miRNAs.

(G) Raising Dicer expression reduces metastatic lung colonization. SCID mice were orthotopically injected in the fat pad with control 4T1 cells or two independent Dicer-expressing lines (n = 6 mice for each cell line). Lungs were explanted after 20 days and scored for the presence of metastases as in (C).

(H and I) representative H&E sections of the lung parenchyma from mice bearing tumors originating from control 4T1 cells (H) or Dicer-expressing 4T1 cells (I).

See also Figure S5.

expressing *miR-107* (Figure 6B). EMT was also validated by gene expression analysis: in the presence of *miR-107*, expression of *E-Cadherin* mRNA was downregulated whereas the mesenchymal markers *vimentin*, *ICAM-1*, and *fibronectin* mRNAs were significantly increased (Figures 6C–6F). In agreement with the role of Dicer downregulation as mediator of *miR-107* effects, lowering Dicer levels by shRNA similarly caused reduction of *E-Cadherin* and induction of *vimentin*. Thus, the ability to induce EMT parallels with the previously shown induction of cell motility by *miR-107* or Dicer downregulation (see Figure S4F).

We next asked if modulating the levels of *miR-103/107* altered the mesenchymal traits of metastatic cells. For this, we monitored the effects of gain and loss of *miR-103/107* in MDA-MB-231. Gain of *miR-107* massively induced expression of *fibronectin*, *vimentin*, and *ICAM* (Figure 6G), whereas antagomiR-mediated depletion of endogenous *miR-103/107* reduced expression of the same genes (Figure 6H).

In line with such an endogenous role of *miR-103/107* in EMT, we found that high versus low levels of *pri-miR-103* are associated with mesenchymal versus epithelial phenotypes in a panel of breast cancer cell lines previously stratified according to expression profiles and metastatic capacity (Charafe-Jauffret et al., 2009) (Figure 6I).

Taken together, the data indicate that expression of *miR-103/107* is sufficient for inducing epithelial plasticity and required for maintenance of mesenchymal gene expression.

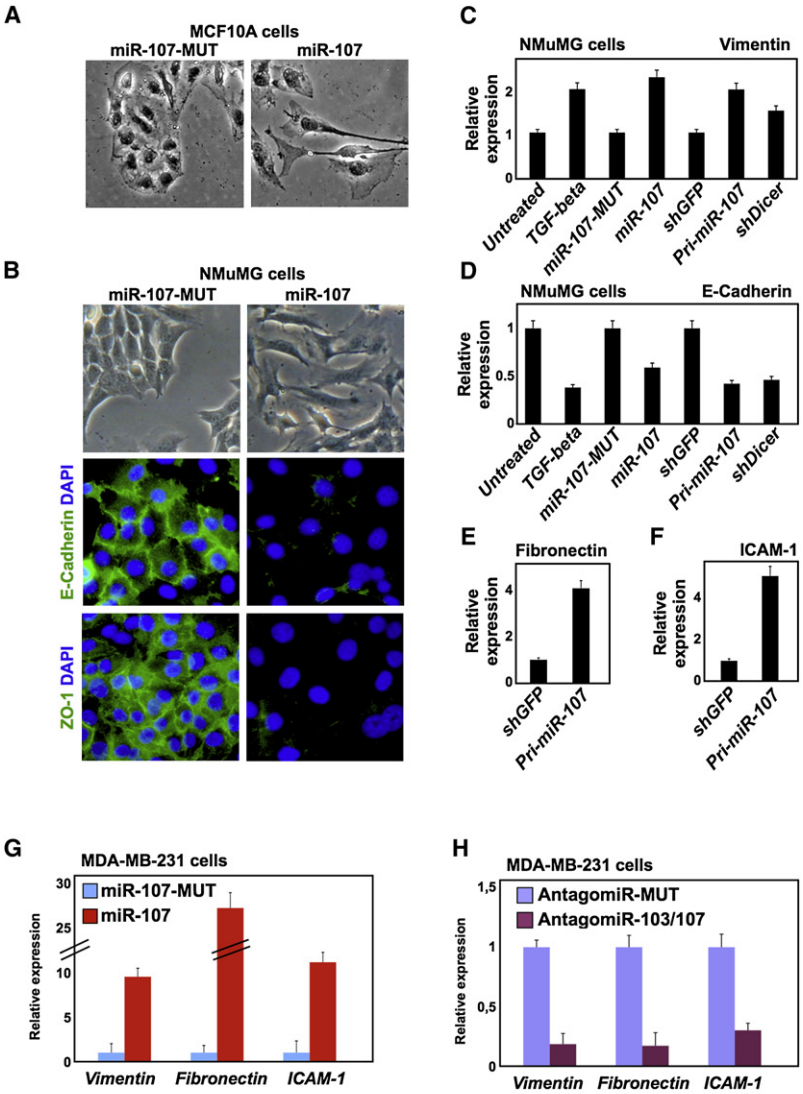

Figure 6. *miR-103/107* Induce Epithelial Plasticity

(A) Morphology of MCF10A cells transiently transfected with mature *miR-107* or the control miRNA (*miR-107-MUT*). Note the loss of cell-cell adhesion and acquisition of spindle morphology in cells expressing *miR-107*.

(B) NMuMG cells were transiently transfected with control miRNA (*miR-107-MUT*) or *miR-107* and, after 3 days, analyzed for epithelial characters. Panels show the bright-field morphology of transfected cells (upper panels) and the immunofluorescence for the adherent junction marker E-Cadherin (green, middle panels) or for the tight junction marker ZO-1 (green, lower panels). Nuclei are stained in blue with DAPI.

(C–F) Expression of the epithelial marker *E-cadherin* (D) and of the mesenchymal markers *vimentin* (C), *fibronectin* (E), and *ICAM-1* (F) was examined by qRT-PCR in NMuMG cells. Graphs show relative expression levels, normalized to *GAPDH*. Stable expression of *pri-miR-107* by retroviral transduction, transient transfection of mature *miR-107*, or shRNA knockdown of Dicer (shDicer) upregulates mesenchymal while inhibiting epithelial markers. *miR-107-MUT* and shGFP are negative controls. TGF-beta treatment (TGFβ1 200 pM for 3 days) serves as positive control for EMT induction. Data are shown as mean and SD.

(G) Transient transfection of mature *miR-107* increases the expression of the mesenchymal markers *vimentin*, *fibronectin*, and *ICAM-1* in MDA-MB-231 cells, as quantified by qRT-PCR. Expression values were given as relative to those of miR-107-MUT-treated cells. Data are shown as mean and SD.

(H) *Pri-miR-103/107* are required to support mesenchymal gene expression in MDA-MB-231 cells. Cells were treated for 5 days with antagomiR-MUT or antagomiR-103/107 and analyzed for mesenchymal markers by qRT-PCR. For each marker, expression values were given as relative to those of antagomiR-MUT-treated cells. Data are shown as mean and SD.

(I) *Pri-miR-103* expression correlates with mesenchymal traits in a panel of breast cancer cell lines. Heatmap depicts the relative changes of standardized expression values of *E-cadherin*, *vimentin*, and *pri-miR-103* for each cell line. Blue indicates low expression whereas yellow indicates high expression.

miR-103/107 Control Mesenchymal Traits by Regulating the Expression of the *miR-200* Family of miRNAs

We next wished to define the identity of key miRNAs acting as downstream mediators of the *miR-103/107*-Dicer axis. We focused on the *miR-200* family (Figure 7A) because previous studies showed that these miRNAs display properties opposite to those of *miR-103/107*: they are required to suppress EMT and migration while their attenuation unleashes mesenchymal gene expression (Inui et al., 2010; Polyak and Weinberg, 2009).

If members of the *miR-200* family are functionally relevant downstream of *miR-103/107*, then *miR-200* should oppose *miR-107*. Confirming this hypothesis, transfection of *miR-200*b in NMuMG cells reverts the EMT induced by *miR-107*, as assayed by morphology and gene expression (Figures 7B and 7C). Migration of MDA-MB-231 cells is inhibited by antagomiR-103/107 but, remarkably, this has no effect in *miR-200*-depleted cells (by means of antago-*miR-200*, targeting the whole *miR-200* family) (Figure 7D).

Biochemically, mature *miR-200* levels were increased by antagomiR-103/107 (Figure 7E). To confirm that this extent of *miR-200* upregulation was biologically effective, we monitored the *miR-200* targets *ZEB1* and *ZEB2*. We found that these genes were downregulated (Figure 7F) in antagomiR-103/107-treated cells to about 50%, mimicking the effect of mature *miR-200* overexpression (see Figure 7I). In agreement, we found that

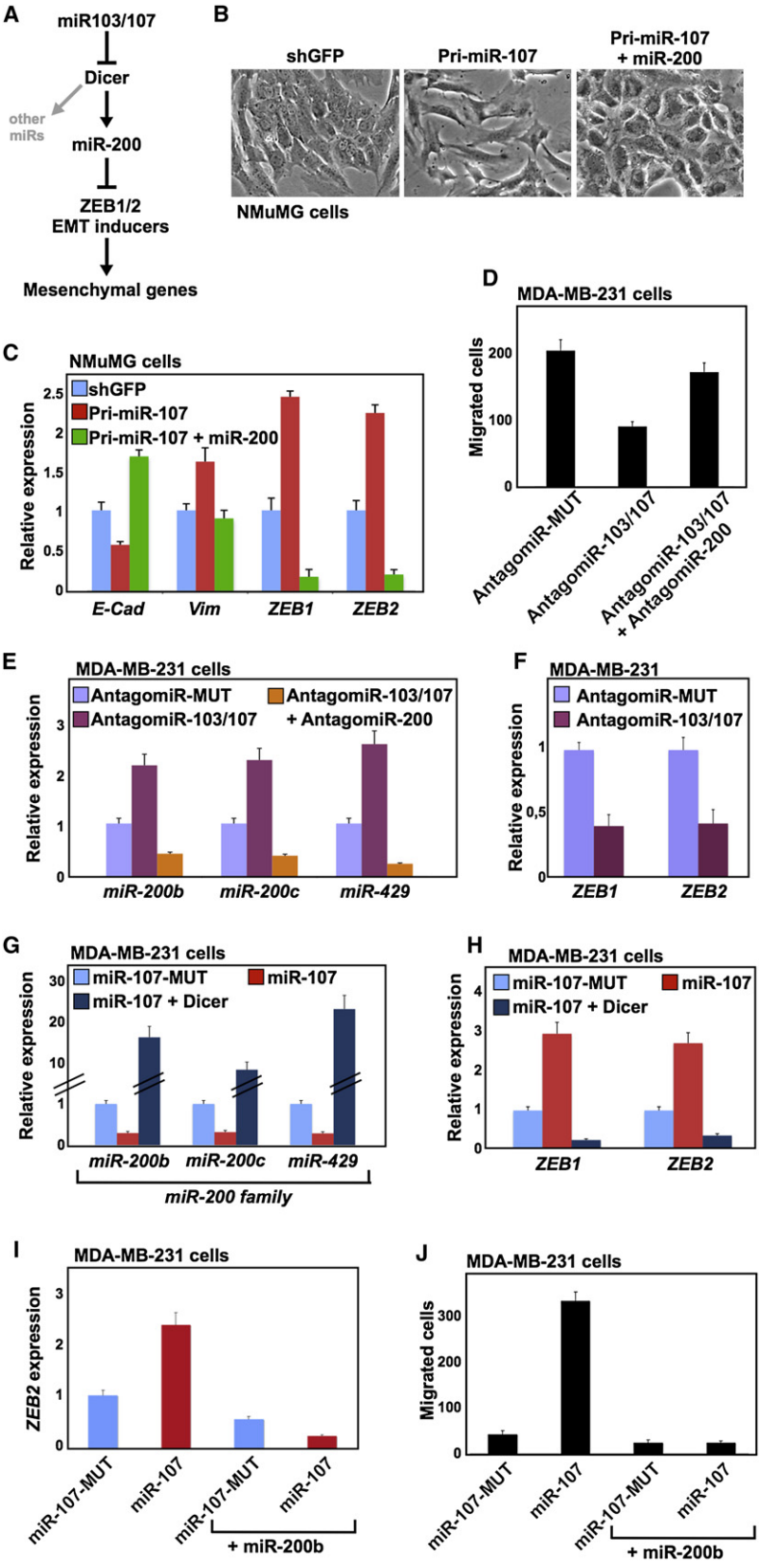

Figure 7. The *miR-200* Family Members Are Inhibited by *miR-103/107* to Promote Mesenchymal Traits

(A) A model for the *miR-103/107*-Dicer-*miR-200* pathway in EMT control.

(B and C) Transfection of *miR-200b* reverts the EMT induced by *pri-miR-107* in NMuMG, as assayed by cell morphology (B) and by qRT-PCR for the expression of epithelial (*E-cadherin*) or mesenchymal markers (*vimentin*, *ZEB1*, and *ZEB2*) (C). Graphs show relative expression levels.

(D) Transwell migration assays of MDA-MB-231 cells treated with antagomiR-103/107, alone or in combination with a mix of antagomiRs targeting the entire *miR-200* family (antagomiR-200). AntagomiR-MUT serves as negative control. Depletion of *miR-103/107* inhibits MDA-MB-231 cell migration but has no effect in cells depleted of the *miR-200* family. See Figure S6A for controls of antagomiR-200 effects.

(E–H) *miR-103/107* regulate the expression and activity of the *miR-200* family.

(E) Expression of mature *miR-200* family members (*miR-429*, *miR-200b*, and *miR-200c*) in MDA-MB-231 cells treated as in (D). Graphs show quantification of gene expression by qRT-PCR. For each marker, expression values were given as relative to those of antagomiR-MUT-treated cells.

(F) qRT-PCR analysis for the expression of the *miR-200* direct targets *ZEB1* and *ZEB2* in MDA-MB-231 cells treated with antagomiR-MUT or antagomiR-103/107.

(G and H) Panels show qRT-PCR for mature *miR-200* family members (G) and for their targets *ZEB1* and *ZEB2* (H) in MDA-MB-231 cells transiently transfected with *miR-107*-MUT or *miR-107*. Coexpression of a miR-insensitive form of *Dicer* transgene opposes the effects of *miR-107*. See Figure S6B for pre-miRNA levels upon *miR-107* transfection.

(I and J) Forced expression of *miR-200b* inhibits the effects of gain of *mir-107* on gene expression and cell migration. MDA-MB-231 cells were transiently transfected with the indicated combinations of miRNAs and assayed for *ZEB2* expression by qRT-PCR (I) or for cell migration by transwell assay (J).

Data are shown as mean and SD. See also Figure S6.

overexpression of *miR-107* downregulates *miR-200* and upregulates *ZEB1* and *ZEB2* mRNA levels (Figures 7G and 7H). Importantly, these effects are potently rescued by adding-back Dicer (Figures 7G and 7H). Crucially, expression of *miR-200* blocks the phenotypic effects of *miR-107*, as assayed by expression of *ZEB2* and cell migration (Figures 7I and 7J), indicating that inhibition of *miR-200* is critical for maintenance of mesenchymal and motile properties by the *miR-103/107*-Dicer axis.

DISCUSSION

The *miR-103/107*-Dicer Connection in Metastasis

The findings here presented provide evidence that cancer cells use global downregulation of the miRNA network to induce epithelial plasticity and foster invasive and metastatic behaviors. In breast cancer, a microRNA targeting Dicer, *miR-103/107*, plays a causal role in these events.

These data contribute to an unsettled issue in cancer biology. Genetically, as revealed by knockout of *Dicer* or *Drosha* in mice, miRNA biosynthesis is essential for basic cellular functions, such as stemness, cell-cycle progression, and mitosis (Bernstein et al., 2003; Fukagawa et al., 2004; Tang et al., 2007); these processes are ostensibly essential at all stages of tumorigenesis. Despite this, global downregulation of miRNA expression and processing appears a widespread phenomenon in cancer (Lu et al., 2005; Ozen et al., 2008; Ventura and Jacks, 2009). These observations beg the question of how cancer cells can seamlessly reconcile to lose miRNA activity without tackling cellular basal functions.

This study unveils a means by which breast cancer cells solve this dilemma. We find that in metastatic cells, high levels of *miR-103/107* attenuate Dicer expression: this empowers invasive and metastatic properties without major impact on primary tumor growth. Thus, it appears that distinct cellular functions are differentially sensitive to Dicer fluctuations. *mir-103/107* keep Dicer below a threshold required for metastasis protection. Conversely, the miRNA network sustaining tumor growth operates safely at lower Dicer levels (Kumar et al., 2009). An appeal of this system is its embedded robustness: *miR-103/107* are both generated by, and regulators of, Dicer; this mutual feedback relationship allows scale-down of Dicer levels but is also intrinsically incompatible with complete depletion, maintaining sufficient Dicer for growth control and, likely, other cellular functions.

miR-103/107 and Epithelial Plasticity

Our clinical validation studies reveal that high levels of *miR-103/107* earmark primary breast tumors with metastatic capacity. By facilitating the acquisition of a more plastic epithelial state, the *miR-103/107*-Dicer axis may assist early tumor dissemination, preceding or conspiring with other genetic lesions that complete neoplastic conversion or endow distant colonization. Moreover, miRNAs have been envisioned as key players in "robustness loops" that prevent aberrant/ectopic gene expression, in so doing stabilizing cell identity and masking expression of genetic variation (Hornstein and Shomron, 2006; Inui et al., 2010). Thus, escaping miRNA control in cancer cells, as attained upon Dicer downregulation, may allow the phenotypic emergence of more aggressive genetic variants, accelerating cancer progression.

A significant finding was indeed the association of the *miR-103/107*-Dicer pair with EMT. In normal tissues, the EMT program is used to assist epithelial plasticity whereas it is exploited opportunistically in cancer to habilitate metastasis (Polyak and Weinberg, 2009). Thus, the ability of *miR-103/107* to turn on this program may well represent a leading mechanism by which *miR-103/107* foster breast cancer metastasis.

It is worth discussing why only EMT becomes manifest after the general downregulation of miRNAs induced by the *miR-103/107*-Dicer axis. For several biological processes, downregulation of miRNAs might not reveal immediate phenotypic consequences in virtue of the "balancing effect" between miRNAs favoring and opposing the same process, keeping the system in equilibrium; for example, increase of *miR-103/107* downregulates miRNAs playing both positive (i.e., *miR-17∼92* cluster or *miR-21*) and negative (i.e., *let-7* family) effects on proliferation (Ventura and Jacks, 2009). In contrast, the gene network controlling the maintenance of the epithelial phenotype appears mainly under positive control by miRNAs, as attested by multiple miRNAs inhibiting EMT (*miR-200*a, *miR-200*b, *miR-200*c, *miR-141*, *miR-429, miR-205*, and *miR-125a)* (Inui et al., 2010; Polyak and Weinberg, 2009). Our data suggest that this imbalance is exploited in breast cancer to favor acquisition of mesenchymal traits. Notably, leading targets of the *miR-200* family are *ZEB1* and *ZEB2*, pivotal genes for mesenchymality (Burk et al., 2008; Liu et al., 2008).

Additionally, the EMT bias can be also explained by the fact that different mRNAs may display differential sensitivity to the changes in levels of cognate miRNAs imposed by *miR-103/107*. From this perspective, it's worth noticing that *miR-200* genes are transcriptionally repressed by ZEB1. This configures an unusual double-negative circuit that magnifies fluctuations in its components, favoring a "switch-like" transition between two alternative states (i.e., epithelial versus fully mesenchymal) (Inui et al., 2010). Indeed, we found that levels of *ZEB1/ZEB2* are controlled by *miR-107* in a *miR-200*-dependent manner (Figures 7F and 7I). As comparison, mature *miR-15/16* and *let-7* family members and *miR-17∼92* cluster are downregulated similarly to *miR-200* by *miR-107*, but the steady-state levels of some of their key targets (*BCL2*, *KRas*, and *cMyc*, respectively) are not affected (Figure S6C). Clearly, our focus on EMT does not exclude that *miR-103/107* may regulate other biological processes regulated by Dicer and miRNAs in metastatic cancer cells or other cellular contexts.

Clinical Implications

In human primary breast tumors, we validated expression of *miR-103/107*, but not *Dicer* mRNA, as prognostic marker. This finding is consistent with *miR-103/107* targeting Dicer translation; this endows *miR-103/107* with a better patient stratification capacity than *Dicer* transcripts. That said, tumors may regulate Dicer by other means, including genetic inactivation; indeed low levels of *Dicer* are associated with poor survival in a fraction of lung and ovarian cancer patients and animal models (Kumar et al., 2009; Karube et al., 2005; Merritt et al., 2008). Here we found that, similarly to elevated *miR-103/107*, heterozygous

loss of *Dicer* also instills metastatic propensity in breast cancer patients. Likely, this result is not apparent from the analysis of *Dicer* mRNA levels because this genetic lesion occurs in a relatively minor fraction of patients, complicating in large datasets the assignments of reliable cutoff values for patients' correlations. It is tempting to speculate that the use of a *miR-103/107* may be preferred over genetic deletion because it may represent a reversible and dynamic means to attenuate Dicer protein levels, perhaps corresponding to a physiological process requiring transient empowering of cell motility (i.e., during wound-healing or neural crest biology).

Finally, our findings have some implications for treatment of breast cancer. The positive effects of antagomiR-103/107 in our experimental models of metastasis at least suggest that modulation of *miR-103/107* by RNA-based therapeutics may prove clinically useful.

EXPERIMENTAL PROCEDURES

Biological Assays in Mammalian Cells

For Transfection procedures and luciferase assays, see the Extended Experimental Procedures and Martello et al., 2007. For wound-healing experiments, cells were plated in 6-well plates, transfected as indicated, and cultured to confluency. Cells were serum-starved and scraped with a P200 tip (time 0), and the number of migrating cells were counted from pictures (five fields) taken at the indicated time points.

Transwell migration/invasion assays were performed in 24-well PET inserts (Costar 8.0 mm pore size). Cells were plated and transfected with miRNA as indicated. The day after, 100.000 cells were plated in serum-free media in transwell inserts (at least three replicas for each sample). Medium containing 1% FBS served as chemoattractant in the lower chamber. Cells in the upper part of the transwell were removed with a cotton swab; migrated cells were fixed in 4% PFA and stained with 0.5% Crystal Violet. Filters were photographed and the total number of cells counted. Each experiment was repeated at least three times independently.

For Dicer knockdown the sequences of the siRNA were: 5′-UCC AGA GCU GCU UCA AGC ATT-3′ and 5′-UGC UUG AAG CAG CUC UGG ATT-3′. As for mature miRNAs: *miR-107*: 5′-AGC AGC AUU GUA CAG GGC UAU CA-3′ and 5′-AUA GCC CUG UAC AAU GCU GCC UU-3′; *miR-107*-MUT: 5′-AUA GCC CUG UAC AuU cCg GaC UU-3′ and 5′-AuC cGg AaU GUA CAG GGC UAU CA-3′; *miR-200*b: 5′-AUC AUU ACC AGG CAG UAU UAG A-3′ and 5′-UAA UAC UGC CUG GUA AUG AUG A-3′.

Experimental Models of Metastasis and AntagomiR-Treatment

Mice were housed in Specific Pathogen Free (SPF) animal facilities and treated in conformity with institutional guidelines. For xenograft studies of breast cancer metastasis, cells (500.000 cells/mouse for 4T1 cells, 1.000.000 cells/mouse for SUM149 cells) were unilaterally injected into the mammary fat pad, or in the tail vein, of SCID female mice, age-matched between 5 and 7 weeks. After the indicated periods, mice were sacrificed and their lungs explanted for histological analyses.

AntagomiRs were designed as described (Krutzfeldt et al., 2005) and purchased from Fidelity System. Sequences were "Antago*miR-103/107*": 5′-U*U*CAU AGCCCUGUACAAUGCUG*C*U*U*-Chol-3′; "AntagomiR-MUT": 5′-U*U*CAUAa CCCUGUAaAAUcaUc*a*U*U*-Chol-3′; "AntagomiR-200a": 5′-G*A*ACATCGT TACCAGCCAGTGT*T*A*G*-Chol-3′; "AntagomiR-200b": 5′-C*C*C ATCCTTA CCCGGCAG TCTT*A*G *A*-Chol-3′; all the bases are 2′-OMe modified, * represents a phosphorothioate linkage, and "Chol" represents linked cholesterol tail. For AntagomiR-200 we used a 1:1 mixture of the two oligos.

4T1 cells, after 4 days of AntagomiR treatment, were orthotopical injected in SCID mice (500.000 cells/mouse). After 3 days, 100 μl of Antago*miR-103/107* or control AntagomiR-MUT solutions (diluted in PBS at 2 mg/ml) were injected intratumorally three times per week for 2 weeks.

SUPPLEMENTAL INFORMATION

Supplemental Information includes Extended Experimental Procedures, six figures, and two tables and can be found with this article online at doi:10.1016/j.cell.2010.05.017.

ACKNOWLEDGMENTS

This work is supported by Cariparo Foundation Excellence-grant and Carimodena Foundation international grants to S.B., and AIRC, University of Padua Strategic-grant, Cariparo Foundation Excellence-grant, IIT (Italian Institute of Technology), and Telethon grants to S.P., and ISSN "Giovani Ricercatori" to G.M. We thank T. Rodriguez, O. Wessely, and D. Volpin for comments on the manuscript; the anonymous reviewers for thoughtful directions; and S. Bobisse and R. Venerando for help with cytofluorimeter. We are grateful to colleagues for gifts of reagents: L. Naldini (lentiviral vectors), T. Jacks (mouse shDicer plasmid), P. Provost (Dicer cDNA), W. Filipowicz (Dicer antibody), R. Agami (miR-Vec), F. Miller (4T1 cells), G. Hannon (Dicer null cells), and R. Weinberg (SUM149 cells).

Received: August 21, 2009
Revised: February 23, 2010
Accepted: April 14, 2010
Published: June 24, 2010

REFERENCES

Ambros, V. (2004). The functions of animal microRNAs. Nature *431*, 350–355.

Aslakson, C.J., and Miller, F.R. (1992). Selective events in the metastatic process defined by analysis of the sequential dissemination of subpopulations of a mouse mammary tumor. Cancer Res. *52*, 1399–1405.

Bartel, D.P. (2009). MicroRNAs: target recognition and regulatory functions. Cell *136*, 215–233.

Baskerville, S., and Bartel, D.P. (2005). Microarray profiling of microRNAs reveals frequent coexpression with neighboring miRNAs and host genes. RNA *11*, 241–247.

Bernstein, E., Kim, S.Y., Carmell, M.A., Murchison, E.P., Alcorn, H., Li, M.Z., Mills, A.A., Elledge, S.J., Anderson, K.V., and Hannon, G.J. (2003). Dicer is essential for mouse development. Nat. Genet. *35*, 215–217.

Burk, U., Schubert, J., Wellner, U., Schmalhofer, O., Vincan, E., Spaderna, S., and Brabletz, T. (2008). A reciprocal repression between ZEB1 and members of the miR-200 family promotes EMT and invasion in cancer cells. EMBO Rep. *9*, 582–589.

Calin, G.A., and Croce, C.M. (2006). MicroRNA signatures in human cancers. Nat. Rev. Cancer *6*, 857–866.

Charafe-Jauffret, E., Ginestier, C., Iovino, F., Wicinski, J., Cervera, N., Finetti, P., Hur, M.H., Diebel, M.E., Monville, F., Dutcher, J., et al. (2009). Breast cancer cell lines contain functional cancer stem cells with metastatic capacity and a distinct molecular signature. Cancer Res. *69*, 1302–1313.

Filipowicz, W., Bhattacharyya, S.N., and Sonenberg, N. (2008). Mechanisms of post-transcriptional regulation by microRNAs: are the answers in sight? Nat. Rev. Genet. *9*, 102–114.

Friedman, R.C., Farh, K.K., Burge, C.B., and Bartel, D.P. (2009). Most mammalian mRNAs are conserved targets of microRNAs. Genome Res. *19*, 92–105.

Fukagawa, T., Nogami, M., Yoshikawa, M., Ikeno, M., Okazaki, T., Takami, Y., Nakayama, T., and Oshimura, M. (2004). Dicer is essential for formation of the heterochromatin structure in vertebrate cells. Nat. Cell Biol. *6*, 784–791.

Hornstein, E., and Shomron, N. (2006). Canalization of development by microRNAs. Nat. Genet. Suppl. *38*, S20–S24.

Inui, M., Martello, G., and Piccolo, S. (2010). microRNA control of signal transduction. Nat. Rev. Mol. Cell Biol. *11*, 252–263.

Karube, Y., Tanaka, H., Osada, H., Tomida, S., Tatematsu, Y., Yanagisawa, K., Yatabe, Y., Takamizawa, J., Miyoshi, S., Mitsudomi, T., et al. (2005). Reduced

expression of Dicer associated with poor prognosis in lung cancer patients. Cancer Sci. *96*, 111–115.

Krek, A., Grun, D., Poy, M.N., Wolf, R., Rosenberg, L., Epstein, E.J., MacMenamin, P., da Piedade, I., Gunsalus, K.C., Stoffel, M., et al. (2005). Combinatorial microRNA target predictions. Nat. Genet. *37*, 495–500.

Krutzfeldt, J., Rajewsky, N., Braich, R., Rajeev, K.G., Tuschl, T., Manoharan, M., and Stoffel, M. (2005). Silencing of microRNAs in vivo with 'antagomirs'. Nature *438*, 685–689.

Kumar, M.S., Lu, J., Mercer, K.L., Golub, T.R., and Jacks, T. (2007). Impaired microRNA processing enhances cellular transformation and tumorigenesis. Nat. Genet. *39*, 673–677.

Kumar, M.S., Pester, R.E., Chen, C.Y., Lane, K., Chin, C., Lu, J., Kirsch, D.G., Golub, T.R., and Jacks, T. (2009). Dicer1 functions as a haploinsufficient tumor suppressor. Genes Dev. *23*, 2700–2704.

Leibovitz, A., Stinson, J.C., McCombs, W.B., 3rd, McCoy, C.E., Mazur, K.C., and Mabry, N.D. (1976). Classification of human colorectal adenocarcinoma cell lines. Cancer Res. *36*, 4562–4569.

Liu, Y., El-Naggar, S., Darling, D.S., Higashi, Y., and Dean, D.C. (2008). Zeb1 links epithelial-mesenchymal transition and cellular senescence. Development *135*, 579–588.

Lu, J., Getz, G., Miska, E.A., Alvarez-Saavedra, E., Lamb, J., Peck, D., Sweet-Cordero, A., Ebert, B.L., Mak, R.H., Ferrando, A.A., et al. (2005). MicroRNA expression profiles classify human cancers. Nature *435*, 834–838.

Ma, L., Teruya-Feldstein, J., and Weinberg, R.A. (2007). Tumour invasion and metastasis initiated by microRNA-10b in breast cancer. Nature *449*, 682–688.

Martello, G., Zacchigna, L., Inui, M., Montagner, M., Adorno, M., Mamidi, A., Morsut, L., Soligo, S., Tran, U., Dupont, S., et al. (2007). MicroRNA control of Nodal signalling. Nature *449*, 183–188.

Merritt, W.M., Lin, Y.G., Han, L.Y., Kamat, A.A., Spannuth, W.A., Schmandt, R., Urbauer, D., Pennacchio, L.A., Cheng, J.F., Nick, A.M., et al. (2008). Dicer, Drosha, and outcomes in patients with ovarian cancer. N. Engl. J. Med. *359*, 2641–2650.

Miettinen, P.J., Ebner, R., Lopez, A.R., and Derynck, R. (1994). TGF-beta induced transdifferentiation of mammary epithelial cells to mesenchymal cells: involvement of type I receptors. J. Cell Biol. *127*, 2021–2036.

Ozen, M., Creighton, C.J., Ozdemir, M., and Ittmann, M. (2008). Widespread deregulation of microRNA expression in human prostate cancer. Oncogene *27*, 1788–1789.

Polyak, K., and Weinberg, R.A. (2009). Transitions between epithelial and mesenchymal states: acquisition of malignant and stem cell traits. Nat. Rev. Cancer *9*, 265–273.

Tang, F., Kaneda, M., O'Carroll, D., Hajkova, P., Barton, S.C., Sun, Y.A., Lee, C., Tarakhovsky, A., Lao, K., and Surani, M.A. (2007). Maternal microRNAs are essential for mouse zygotic development. Genes Dev. *21*, 644–648.

Ventura, A., and Jacks, T. (2009). MicroRNAs and cancer: short RNAs go a long way. Cell *136*, 586–591.

Volinia, S., Calin, G.A., Liu, C.G., Ambs, S., Cimmino, A., Petrocca, F., Visone, R., Iorio, M., Roldo, C., Ferracin, M., et al. (2006). A microRNA expression signature of human solid tumors defines cancer gene targets. Proc. Natl. Acad. Sci. USA *103*, 2257–2261.